

## Fine and superfine structure of Decameter-Hectometer type II burst on 2011 June 7

V. V. Dorovskyy<sup>1</sup> · V. N. Melnik<sup>1</sup> ·  
A. A. Konovalenko<sup>1</sup> · A. I. Brazhenko<sup>2</sup> ·  
M. Panchenko<sup>3</sup> · S. Poedts<sup>4</sup> ·  
V. A. Mykhaylov<sup>5</sup>

© Springer ●●●●

### Abstract

The characteristics of the type II bursts with herringbone structure observed both by ground based radio telescopes (UTR-2, URAN-2) and spaceborn spectrometers (STEREO A-B) are discussed. The burst was recorded on 7 June, 2011 in the frequency band 3–33 MHz. It was characterized by extremely rich fine structure. The statistical analysis of more than 300 herringbone sub-bursts constituting the burst was performed separately for the positively (reverse) and negatively (forward) drifting sub-bursts. The sense and the degree of circular polarization of the herringbone sub-bursts were measured in the respectively wide frequency band (16–32 MHz). A second order fine frequency structure of the herringbone sub-bursts was firstly observed and processed. Using STEREO COR1 (A,B) and SOHO LASCO C2 images the direction and radial speed of the CME responsible for the studied type II burst were determined. The possible location of the type II burst source on the flank of the shock was found.

**Keywords:** Corona, Structures, Coronal Mass Ejections, Radio Bursts, Type II, Meter-Wavelengths and Longer (m, dkm, hm, km), Dynamic Spectrum

### 1. Introduction

The beginning of the 24-th solar cycle was accompanied by the increased rate of high energy transients, such as Coronal Mass Ejections (CME). It looks natural since CMEs are considered to be tightly connected with the solar flares (Yashiro *et al.*, 2008) and the flare occurrence rate is the signature of the solar

---

<sup>1</sup> Institute of Radio Astronomy email:  
dorovsky@rian.kharkov.ua

<sup>2</sup> Poltava Gravimetric Observatory email: brazhai@gmail.com

<sup>3</sup> Space Research Institute email:  
mykhaylo.panchenko@oeaw.ac.at

<sup>4</sup> University KU Leuven email:  
Stefaan.Poedts@wis.kuleuven.be

<sup>5</sup> Karazin National University

---

activity. CMEs belong to the class of events which play the key role in the space weather forming. One of the CME signatures in radio band are type II bursts. It is currently accepted that type II bursts are generated by sub-relativistic electrons accelerated at the front of the shocks driven by CMEs (Zajtsev *et al.*, 1998; Mann and Klassen, 2005; Miteva and Mann, 2007). Type II bursts are observed in the wide frequency range from decimeter (dm) through meter (m) and decameter-hectometer (DH) down to kilometer (km) wavelengths bands. In frames of the plasma emission mechanism this fact proves the existence of shocks at the heliocentric distances from one solar radius up to 1 AU. At high frequencies (e.g. dm and m bands) type II burst may also be connected with the flare-generated blast waves without associated CMEs (Magdalenić *et al.*, 2012). But observations show that these flare-generated shocks are characterized by fast deceleration and dissipation (Vršnak and Cliver, 2008) and hence cannot propagate high in the corona. At the same time type II bursts which can be traced consequently in m, DH bands and lower are connected with shocks driven by CMEs of extremely high kinetic energy thus being potentially the most geoeffective events (Gopalswamy *et al.*, 2005).

From this point of view and taking into account the possibility of ground based observations with excellent sensitivity and resolutions, the detailed study of type II bursts parameters in the decameter wavelengths band is of great scientific interest.

Special attention should be focused on study of type II bursts with so called "herringbone" (or simply "HB") structure since they give the most obvious manifestation of the electrons acceleration at the shock front (Zajtsev *et al.*, 1998).

The HB structure was discovered and described by (Roberts, 1959) in meter wavelengths band. The term "herringbone" comes from the morphology of the dynamic spectrum of the burst, representing the positively and negatively drifting short sub-bursts diverging from the main backbone towards higher and lower frequencies respectively and reminding the fish-bone. The type II bursts with HB structure are not rare events. Cane and White (1989) stated that in average 21% of all type II population exhibit HB structure. They also noted that the HB structure occurrence rate is strongly correlated with the intensity. They also remarked that in a group of intense type IIs as many as 60% of them have HB structure. HB structure as well as normal type II bursts exhibit fundamental and harmonic emission. Fundamental HB sub-bursts are more intense and more strongly polarized than the fundamental ones, unlike the maternal type II burst, whose fundamental emission is weaker and both harmonics are almost unpolarized (Cairns and Robinson, 1987). Suzuki, Stewart, and Magun (1980) noted also that negatively drifting HB sub-bursts tended to have higher degree of circular polarization than the positively drifting ones.

## 2. Observations and analysis

In summer months 2011 the observations of the solar sporadic radio emissions were performed by two Ukrainian decameter radio telescopes: the UTR-2 radio telescope (Southern arm with collecting area  $\approx 50000 \text{ m}^2$ ) (Braude *et al.*, 1978)

---

and the URAN-2 array with total collecting area of  $\approx 28000 \text{ m}^2$  (Brazhenko *et al.*, 2005). Since the URAN-2 telescope consisted of cross-dipoles it allowed measuring the sense and the degree of circular polarization of the radio emission. Both radio telescopes operated in frequency range 8 – 32 MHz and were equipped with similar up-to-date back-ends. Dual channel spectropolarimeter DSPZ performed real time 8192-point FFT each 120  $\mu\text{s}$  and provided real time polarization degree calculations. The two telescopes were separated by  $\approx 150 \text{ km}$  that allowed to exclude the effect of the ionosphere.

For the analysis we have selected the type II bursts observed on 7 June 2011. This burst was registered by both the ground based and spaceborn radio telescopes in frequency band 3–32 MHz. The type II burst itself was a part of more complex and large-scale event which apparently was initiated by the powerful solar M2 flare occurred at 06:20 UT near NOAA11226 active region (S22W52).

The dynamic spectrum of the whole complex event observed by URAN-2 and UTR-2 radio telescopes on 7 June 2011 is shown in Figure 1a. The event started at 06:29 UT with a sudden increase of the radio emission continuum by almost 5 orders of the flux magnitude in the whole frequency range covered by the radio telescopes. The continuum jump is marked with *s*. About 90 minutes later a group of powerful type III bursts was registered. Finally, the type II burst with peak fluxes reaching  $10^6 \text{ s.f.u.}$  started at 06:34:00 UT and lasted for about half an hour.

In addition we must note that this type II burst was briefly described by Zucca *et al.* (2012). They made observations in frequency band 20-400 MHz with Callisto spectrograph installed at Rose Solar-Terrestrial Observatory and found that the burst consisted of Fundamental and Harmonic components and was accompanied by moving type IV continuum at frequencies 130-400 MHz. Unfortunately insufficient time and frequency resolution of the experiment did not allow detailed analysis of the rich fine structure of the type II burst. On the contrary UTR-2 and URAN-2 radio telescopes provided data with frequency resolution of 4 kHz and time resolution of 100 ms in frequency bands of 12 – 32 MHz and completely resolve the emission fine structure.

Zoomed fragment of the dynamic spectrum (Figure 1c) unambiguously shows that this burst belongs to the well known class of type II bursts with HB structure since separate sub-bursts of this structure with positive and negative frequency drift rates are clearly seen there. Standard type II bursts of such kind consist of separate “bones” with drift rates of the opposite signs and the “backbone” – the emission lane from which the “bones” seem to start. However there were reports about “backboneless” HB structured type IIs (Holman and Pesses, 1983), when the backbone looks like an emission gap separating the sub-bursts with drifts of the opposite signs. The latter was the case on 7 June 2011.

### 2.1. Frequency drift rate of the type II backbone

Usually the frequency drift rates of the backbone of type II bursts with HB structure are either very low (Melnik *et al.*, 2004) or absent at all (Carley *et al.*, 2013). This fact is commonly explained by the shock wave propagation in non-radial

---

direction, i.e. at the substantial angles ( $> 45^\circ$ ) to the coronal plasma density gradient (Holman and Pesses, 1983; Melnik *et al.*, 2004). The discussed type II burst is out of the common. Its backbone has not only respectively high average frequency drift rate but apparently "wavelike" appearance in the dynamic spectrum as schematically shown in Figure 2b by dashed line.

In the case of monotonous backbone frequency drift (Figure 2a) the drift rate is determined by the radial velocity of the CME-driven shock. In the case of "wavy" backbone (Figure 2b) it is reasonable to estimate average radial velocity of the source by the trend of frequency drift rate along the line representing the linear approximation of the backbone (dotted line in Figure 2b).

For the discussed type II burst the average drift rate is about  $-25$  kHz/s within the frequency bounds 16–25 MHz that corresponds to radial component of the shock front velocity near  $600$  km  $s^{-1}$ . Hereinafter all radial velocities are given for Newkirk corona model. At the same time instant absolute drift rates of separate parts of the backbone sometimes exceed  $100$  kHz  $s^{-1}$ . Totally we have registered 3 full periods of the backbone oscillations between 6:41 UT and 6:57 UT. These periods are 530 s, 230 s and 150 s respectively. The magnitude of these oscillations along frequency axis averaged 10 MHz.

The continuation of the burst at frequencies below 12 MHz was registered by the STEREO/WAVES radio receivers. Identification of the HB structure and thus detection of the backbone in data obtained from the spaceborn receivers was not possible due to bad time resolution (1 min) and insufficient sensitivity. So we derived the total frequency drift rate along the low-frequency edge of the dynamic spectrum (Figure 3).

The obtained drift rates of  $-8$  kHz  $s^{-1}$  at 6 MHz and  $-3$  kHz  $s^{-1}$  at 3 MHz correspond to the linear velocities of 550 and 400 km  $s^{-1}$  respectively.

High frequency and time resolutions of the ground-based back-ends allowed to make detailed statistical analysis of the main parameters of the HB structure sub-bursts. During the life-time of the type-II bursts about 300 separate sub-bursts were identified, 200 of which had negative frequency drift rates (forward sub-bursts) and the rest had positive ones (reverse sub-bursts). The basic parameters of the sub-bursts such as frequency drift rates and durations appeared to be distributed within relatively narrow intervals.

## 2.2. Frequency drift rates of the HB sub-bursts

Total amount of the forward sub-bursts counted 201. The distribution of these sub-bursts by the absolute value of the drift rate is given in Figure 4a. Figure 4b shows corresponding distribution of the reverse sub-bursts.

The average absolute value of the forward sub-bursts drift rates appeared to be equal to  $1.23$  MHz  $s^{-1}$  with maximum of distribution at  $0.8$  MHz  $s^{-1}$ . The distribution is evidently asymmetric with steep slope towards slower drift rates and rather flat fall towards faster ones. This distribution resembles those obtained for forward drift pairs (Melnik *et al.*, 2005) and solar S-bursts (Dorovsky *et al.*, 2006; Briand *et al.*, 2008).

The corresponding distribution of the reverse sub-bursts in general is close to that for forward ones, except the absolute average drift rate which is 1.5 times

---

higher ( $1.8 \text{ MHz s}^{-1}$ ) and maximum of the distribution observed at  $1.4 \text{ MHz s}^{-1}$ . From above figures we may conclude that the drift rates of the HB sub-bursts of one separate type II burst are distributed in a respectively narrow range from  $0.5$  to  $2.5 \text{ MHz s}^{-1}$ , that is slightly slower than drift rates of normal type III bursts in decameter wavelengths band.

Since the HB structure was observed in the respectively wide frequency band, it is of evident interest to investigate the dependence of the absolute drift rates of the sub-bursts on frequency.

The obtained dependences were approximated by the power law empirical equations separately for forward (1) and reverse (2) sub-bursts:

$$\left| \frac{df_f}{dt} \right|_F = 0.01 \cdot f^{1.73}, \quad \text{standard error} = 0.12, \quad (1)$$

$$\left| \frac{df_r}{dt} \right|_R = 0.088 \cdot f, \quad \text{standard error} = 0.15. \quad (2)$$

Here drift rates are given in  $\text{MHz s}^{-1}$  and frequency in  $\text{MHz}$ . The dependence for forward sub-bursts (1) is very close to that derived for type III bursts by Alvarez and Haddock (1973) while the dependence for reverse HB sub-bursts (2) appears to be linear.

### 2.3. Durations of the HB sub-bursts

Another important parameter of the solar radio bursts carrying the information about the properties of the sub-relativistic electron beams is burst duration at fixed frequency. The distribution of the HB sub-bursts by their instant durations is shown in Figure 5. Roughly speaking these distributions are similar. The only difference is the average durations of forward (2.3 s) and reverse (1.9 s) sub-bursts. Both values are substantially smaller than typical durations of the type III bursts.

### 2.4. Polarization of the HB sub-bursts

The URAN-2 radio telescope equipped with the broad-band spectropolarimeter allowed us to detect the sense and the degree of circular polarization of the sub-bursts in the frequency band 16–32  $\text{MHz}$ . Investigations of the HB structure polarization was firstly performed at such low frequencies. The power and polarization spectra are shown in Figure 6.

As was noted earlier (Suzuki, Stewart, and Magun, 1980) the HB structure sub-bursts corresponding to the fundamental emission usually have considerably higher degree of circular polarization in comparison with the polarization degree of the backbone (if it exists) and parent type II bursts. Our observations confirm this fact. Average degree of circular polarization of both kinds of the sub-bursts equaled 50% in some cases reaching as high as 80%. It seems very important that the sense of circular polarization of the forward and reverse sub-bursts appeared to be the same. In all cases the left-handed circular polarization was observed.

---

At the same time the polarization of the preceding powerful type III bursts was of much less degree (20–30%) and of the opposite sense.

### 2.5. Fine frequency structure of the HB sub-bursts

High frequency resolution of the experiment allowed to define a "second order fine structure" of the HB sub-bursts. This fine structure (see Figure 7) has an appearance of the quasi-periodic (in frequency domain) chain of narrow-band sub-bursts. The bandwidths of these sub-bursts were 30–60 kHz and frequency spacing between neighboring sub-bursts were 60–120 kHz. This fine structure is close to the "fringe" structure of solar S-bursts, described in (McConnell, 1982). As a rule the narrow-band sub-bursts had no own drift rate while in rare cases the slight positive drift rates of  $100 \text{ kHz s}^{-1}$  were observed (Figure 7d). The characteristic feature of the first (in time) sub-burst shown in Figure 7d is that the drift rate of the narrow-band sub-bursts changes from  $+150 \text{ kHz s}^{-1}$  at the beginning down to  $20 \text{ kHz s}^{-1}$  at the end of the burst.

### 2.6. The associated solar events

Data obtained from SOHO show that the discussed complex solar burst was the result of the M2 solar flare, taken place near the active region NOAA11226 located in the South-West part of the solar disk ( $22^\circ\text{S}$ ,  $52^\circ\text{W}$ ). According to the GOES data the X-Ray flux was raising from the background level till the maximum point for 8 min, from 06:19 UT till 06:27 UT. Along with it the flux of the background continual solar radio emission was rapidly increasing from quiet Sun level to the value of 10000 s.f.u. for only 9 s – from 06:26:03 till 06:26:12 UT. We must note that the leading edge of this increase had characteristic drift rate of  $-4.5 \text{ MHz s}^{-1}$  from high to low frequencies. It indicates that the discussed continuum raise could be caused by the electrons moving with velocity of  $\sim 10^{10} \text{ cm s}^{-1}$  away from the Sun. The electrons with such velocities are usually associated with normal type III bursts. Approximately in 2 minutes after the continuum raise the dense group of powerful type III bursts started. Taking into account the time needed for electrons to travel from the flare region to the location of the observed radio emission source (at the velocity of  $10^{10} \text{ cm s}^{-1}$  it roughly counts 5 s), we can conclude that acceleration of the electrons responsible for the continuum jump took place during the raising phase of the flare, before X-ray flux reached its maximum. At the same time the electrons which initiated the subsequent type III bursts were accelerated after the flare reached the maximum intensity. We should also note that such a sequence when type II burst is preceded by the group of powerful type III bursts and followed by type IV continuum is observed respectively often.

Using data of COR1 (A and B) coronagraph installed onboard the STEREO satellites it is easy to define that the CME driven shock reached the heliocentric height of  $1.7R_\odot$  with local plasma frequency of 30 MHz at about 06:30 UT. This time corresponds to the onset of the type II bursts at frequency 30 MHz. Since we've got sky-plane images of the CME obtained from 3 different coronagraphs located along the Earth's orbit at approximately  $90^\circ$  angular separation it was

---

possible to retrieve the real absolute velocity and the direction of the CME propagation as shown in Figure 8a. The sky-plane component of the CME velocity obtained from STEREO-A spacecraft ( $V_{STA}$ ) was found to be equal  $1200 \text{ km s}^{-1}$  and accordingly that from SOHO spacecraft ( $V_{SOHO}$ ) equaled  $1550 \text{ km s}^{-1}$ . Solving simple trigonometric equations we obtain the absolute CME velocity ( $V_{CME}$ ) of  $1950 \text{ km s}^{-1}$  and the direction of about  $52^\circ$  westward from the observer's line-of-sight. Apparently the obtained angle coincides with the longitudinal position of the active region NOAA11226 and proves the previously supposed association between the CME and the active region. This fact also agrees with the statement that CMEs preferably propagate in the radial direction above the corresponding active region (Yashiro *et al.*, 2008). At such a velocity the CME would cover 1 AU distance in approximately 20 hours, and thus should arrive to the Earth's orbit around 02:30 UT on 8 June 2011.

It is known that the ability of CME to produce considerable impacts upon the space weather conditions is determined by its basic kinetic properties: the speed, the angular width and the direction (Gopalswamy, 2011). The population of the geoeffective CMEs has average speed of  $\sim 1000 \text{ km s}^{-1}$  and includes mostly halo-CMEs which are in fact normal CMEs propagating towards (or straight away) the Earth (Gopalswamy, 2009). In addition many authors reported (Michalek *et al.*, 2006; Kim *et al.*, 2010) that at all other parameters being equal the CMEs originating from western hemisphere used to cause more intense geomagnetic storms. Discussed halo-CME had all signs of geoeffectiveness except the direction. Nevertheless slight decreasing of the Dst index down to  $-30 \text{ nT}$  in average was registered at the beginning of the 8 June 2011. We suppose that this decrease might be caused by the eastern flank of the CME when it reached the Earth's magnetosphere

At the same time the solar wind parameters deviations were observed by the ACE and GOES spacecraft at the time of the CME possible arrival. Thus, the proton speed increased from  $400$  to  $550 \text{ km s}^{-1}$ , proton temperature raised from  $7 \cdot 10^4 \text{ K}$  to  $2 \cdot 10^5 \text{ K}$  and shortly, for only 5 hours there was a jump in the proton density from  $4$  to  $12 \text{ cm}^{-3}$ .

### 3. Discussion

As it follows from the data analysis the shock linear velocity retrieved from coronagraph observations is at least three times higher than the radial velocity of the radio source derived from the frequency drift rate of the burst ( $1950$  and  $650 \text{ km s}^{-1}$  respectively). In our opinion this discrepancy could take place when the source of the type II bursts was located not at the forehead but at the flank of the shock. Indeed, the drift rate of the bursts is determined by the radial component of the total linear velocity of the source, as

$$D_f = \frac{f}{2} \frac{1}{N} \frac{dN}{dr} \cdot V_s \cdot \cos \theta, \quad (3)$$

where  $f$  is the frequency,  $N$  is the plasma density,  $dN/dr$  is the density gradient,  $V_s$  is the source linear velocity and  $\theta$  is the angle between the density gradient



---

and the source velocity vector. In other words only the radial component of the total source velocity contributes to the frequency drift rate. Moreover the flanks of CME where the emission source is supposed to be located may propagate slower than the CME forehead (Gopalswamy, 2009). Detailed analysis of the SOHO C2 images shows that the radial velocities of the regions, deflected from the forehead direction by approximately 40–50° (in latitudinal plane) are at least one third of the CME forehead speed. Assuming quasi-symmetrical cone-like expansion of the CME (Gopalswamy, 2009) one may suppose the same velocity for the case of longitudinal deflection by the mentioned angle. Taking into account the derived CME propagation direction we conclude that the type II burst may originate from the eastern flank of the shock, which moves non-radially ( $\sim 50^\circ$  to the density gradient) towards the Earth as shown in Figure 8b.

The wavelike oscillations of the backbone was firstly noted by (Melnik *et al.*, 2004). Authors assumed that "waving" could be the result of the shock front intersecting coronal streamer while moving almost normally to the coronal density gradient. Recent investigations, e.g. (Reiner *et al.*, 2003; Feng *et al.*, 2012; Kong *et al.*, 2012), show that the sources of type II radio emissions are likely located at regions where CME flanks intersect dense coronal streamers. This explanation seems reasonable also for the discussed burst. With little corrections that the source apparently moved at the angle about 50° to the CME forehead direction and intersected at least three inhomogeneous regions, most likely streamers. The magnitude of the backbone oscillations in this case is determined by the ratio between plasma density inside the streamer and the ambient coronal plasma density. Thus 10 MHz oscillation magnitude corresponds to the density deviation of  $5 \cdot 10^6 \text{ cm}^{-3}$ . Judging from the periods of the oscillations the linear distance between neighboring streamers are  $0.5 R_\odot$ ,  $0.2 R_\odot$ , and  $0.15 R_\odot$ . Since these distances are determined at the heliocentric heights of about  $2 R_\odot$  the corresponding angular separations between the streamers count  $\sim 10^\circ$ ,  $15^\circ$  and  $25^\circ$ . Then transverse dimensions of the streamers at the mentioned height vary from  $\sim 0.1$  to  $0.2 R_\odot$ .

High degree of circular polarization of the herringbone sub-bursts indicates the fundamental emission. On the contrary the polarization of the accompanying type III has opposite sense. It may indicate that the conditions at the sources regions of the HB and type III bursts are quite different. First of all it concerns the magnetic field direction.

The frequency range over which a separate HB burst extends is rather narrow in comparison with type III bursts. For the observed burst this frequency range varied from 2 to 10 MHz. Taking into account the source velocity derived from the HB bursts drift rates linear dimensions of the area when emission is possible lay between  $3 \cdot 10^9 \text{ cm}$  and  $2 \cdot 10^{10} \text{ cm}$  (or  $0.05 R_\odot$  and  $0.3 R_\odot$ ).

It is commonly assumed the linear velocities of the electron generating the forward and the reverse HB bursts are approximately equal. The difference between mean values of the absolute drift rates of these two populations are more likely caused by different conditions behind and in front of the source position. This fact may also play role in the difference of the drift rates dependences (1) and (2). One can easily note that the dependence for forward HBs is more close to the universal dependence  $D_f = -0.01 \cdot f^{1.84}$  derived by Alvarez and



---

Haddock (1973) for the type III bursts in the undisturbed corona then that for reverse ones. It seems natural since the forward HBs are produced by electrons moving away from the Sun, across the undisturbed yet corona. The electrons propagating towards the Sun meet the after-shock corona and thus the density gradient may be different from that of quiet corona.

#### 4. Conclusion

The detailed analysis of the type II burst observed on 7 June 2011 by three different radio telescopes was performed.

This type II burst occurred in association with the preceding powerful type III bursts, which seem to be initiated by the solar flare near AR11226. The total frequency drift rate of the burst is close to that of ordinary type II. Thus drift rates of HB type II bursts may vary from several tens of kHz per second in the decameter band down to zero. Sometimes such bursts may have no backbone emission and/or have "wavy" backbone. The characteristic sizes of the inhomogeneities, more likely streamers, responsible for the waving in our case laid between 0.1 and 0.5  $R_{\odot}$ .

The discrepancy between visible CME velocity and retrieved from the drift rate type II source radial velocity is explained by: 1 - different velocities of the CME forehead and its flank where the source is supposed to be located and 2 - non-radial propagation of the source.

The statistical analysis of the HB sub-bursts parameters showed that forward HB bursts had slower drift rates ( $-1.23 \text{ MHz s}^{-1}$  in average) and were slightly longer (2.27 s) than the reverse bursts ( $+1.8 \text{ MHz s}^{-1}$  and 1.85 s respectively). In addition the dependence of the drift rates on frequency for forward HB sub-bursts found to be close to well known Alvarez and Haddock (1973) dependence for type III bursts while the drift rates of reverse HB sub-bursts were proportional to the frequency.

The HB structure expectedly appeared to be strongly polarized. Moreover both forward and reverse HB sub-bursts were left-handed polarized. Unlike the preceding type IIIs, whose sense of polarization was opposite.

**Acknowledgements** The work was partially performed under the support of the European FP-7 project SOLSPANET (FP7-People-2010-IRSES-269299). The work of M.P. was supported by the Austrian Fonds zur Frderung der wissenschaftlichen Forschung (project P23762-N16). Conflict of Interest: The authors declare that they have no conflict of interest.

#### References

- Alvarez, H., Haddock, F.T.: 1973, Solar Wind Density Model from km-Wave Type III Bursts. *Solar Phys.* **29**, 197–209. doi:10.1007/BF00153449.
- Braude, S.I., Megn, A.V., Riabov, B.P., Sharykin, N.K., Zhuk, I.N.: 1978, Decametric survey of discrete sources in the Northern sky. I - The UTR-2 radio telescope: Experimental techniques and data processing. *Astrophys. Space Sci.* **54**, 3–36. doi:10.1007/BF00637902.

- Brazhenko, A.I., Bulatsen, V.G., Vashchishin, R.V., Frantsuzenko, A.V., Konovalenko, A.A., Falkovich, I.S., Abranin, E.P., Ulyanov, O.M., Zakharenko, V.V., Lecacheux, A., Rucker, H.: 2005, New decameter radiopolarimeter URAN-2. *Kinematika i Fizika Nebesnykh Tel Supplement* **5**, 43–46.
- Briand, C., Zaslavsky, A., Maksimovic, M., Zarka, P., Lecacheux, A., Rucker, H.O., Konovalenko, A.A., Abranin, E.P., Dorovsky, V.V., Stanislavsky, A.A., Melnik, V.N.: 2008, Faint solar radio structures from decametric observations. *Astron. Astrophys.* **490**, 339–344. doi:10.1051/0004-6361:200809842.
- Cairns, I.H., Robinson, R.D.: 1987, Herringbone bursts associated with type II solar radio emission. *Solar Phys.* **111**, 365–383. doi:10.1007/BF00148526.
- Cane, H.V., White, S.M.: 1989, On the source conditions for herringbone structure in type II solar radio bursts. *Solar Phys.* **120**, 137–144. doi:10.1007/BF00148539.
- Carley, E.P., Long, D.M., Byrne, J.P., Zucca, P., Bloomfield, D.S., McCauley, J., Gallagher, P.T.: 2013, Quasiperiodic acceleration of electrons by a plasmoid-driven shock in the solar atmosphere. *Nature Physics* **9**, 811–816. doi:10.1038/nphys2767.
- Dorovskyy, V.V., Mel’Nik, V.N., Konovalenko, A.A., Rucker, H.O., Abranin, E.P., Lecacheux, A.: 2006, Observations of Solar S-bursts at the decameter wavelengths. In: Rucker, H.O., Kurth, W., Mann, G. (eds.) *Planetary Radio Emissions VI*, 383.
- Feng, S.W., Chen, Y., Kong, X.L., Li, G., Song, H.Q., Feng, X.S., Liu, Y.: 2012, Radio Signatures of Coronal-mass-ejection-Streamer Interaction and Source Diagnostics of Type II Radio Burst. *Astrophys. J.* **753**, 21. doi:10.1088/0004-637X/753/1/21.
- Gopalswamy, N.: 2009, Halo coronal mass ejections and geomagnetic storms. *Earth, Planets, and Space* **61**, 595–597.
- Gopalswamy, N.: 2011, Coronal mass ejections and their heliospheric consequences. In: *Astronomical Society of India Conference Series, Astronomical Society of India Conference Series* **2**, 241–258.
- Gopalswamy, N., Aguilar-Rodriguez, E., Yashiro, S., Nunes, S., Kaiser, M.L., Howard, R.A.: 2005, Type II radio bursts and energetic solar eruptions. *Journal of Geophysical Research (Space Physics)* **110**, 12. doi:10.1029/2005JA011158.
- Holman, G.D., Pesses, M.E.: 1983, Solar type II radio emission and the shock drift acceleration of electrons. *Astrophys. J.* **267**, 837–843. doi:10.1086/160918.
- Kim, R.-S., Cho, K.-S., Moon, Y.-J., Dryer, M., Lee, J., Yi, Y., Kim, K.-H., Wang, H., Park, Y.-D., Kim, Y.H.: 2010, An empirical model for prediction of geomagnetic storms using initially observed CME parameters at the Sun. *Journal of Geophysical Research (Space Physics)* **115**, 12108. doi:10.1029/2010JA015322.
- Kong, X.L., Chen, Y., Li, G., Feng, S.W., Song, H.Q., Guo, F., Jiao, F.R.: 2012, A Broken Solar Type II Radio Burst Induced by a Coronal Shock Propagating across the Streamer Boundary. *Astrophys. J.* **750**, 158. doi:10.1088/0004-637X/750/2/158.
- Magdalenic, J., Marqué, C., Zhukov, A.N., Vršnak, B., Veronig, A.: 2012, Flare-generated Type II Burst without Associated Coronal Mass Ejection. *Astrophys. J.* **746**, 152. doi:10.1088/0004-637X/746/2/152.
- Mann, G., Klassen, A.: 2005, Electron beams generated by shock waves in the solar corona. *Astron. Astrophys.* **441**, 319–326. doi:10.1051/0004-6361:20034396.
- McConnell, D.: 1982, Spectral characteristics of solar S bursts. *Solar Phys.* **78**, 253–269. doi:10.1007/BF00151608.
- Melnik, V.N., Konovalenko, A.A., Rucker, H.O., Stanislavsky, A.A., Abranin, E.P., Lecacheux, A., Mann, G., Warmuth, A., Zaitsev, V.V., Boudjada, M.Y., Dorovskii, V.V., Zaharenko, V.V., Lisachenko, V.N., Rosolen, C.: 2004, Observations of Solar Type II bursts at frequencies 10-30 MHz. *Solar Phys.* **222**, 151–166. doi:10.1023/B:SOLA.0000036854.66380.a4.
- Melnik, V.N., Konovalenko, A.A., Dorovskyy, V.V., Rucker, H.O., Abranin, E.P., Lisachenko, V.N., Lecacheux, A.: 2005, Solar Drift Pair Bursts in the Decameter Range. *Solar Phys.* **231**, 143–155. doi:10.1007/s11207-005-8272-4.
- Michalek, G., Gopalswamy, N., Lara, A., Yashiro, S.: 2006, Properties and geoeffectiveness of halo coronal mass ejections. *Space Weather* **4**, 10003. doi:10.1029/2005SW000218.
- Miteva, R., Mann, G.: 2007, The electron acceleration at shock waves in the solar corona. *Astron. Astrophys.* **474**, 617–625. doi:10.1051/0004-6361:20066856.
- Reiner, M.J., Vourlidas, A., Cyr, O.C.S., Burkepile, J.T., Howard, R.A., Kaiser, M.L., Prestage, N.P., Bougeret, J.-L.: 2003, Constraints on Coronal Mass Ejection Dynamics from Simultaneous Radio and White-Light Observations. *Astrophys. J.* **590**, 533–546. doi:10.1086/374917.

- 
- Roberts, J.A.: 1959, Solar Radio Bursts of Spectral Type II. *Australian Journal of Physics* **12**, 327. doi:10.1071/PH590327.
- Suzuki, S., Stewart, R.T., Magun, A.: 1980, Polarization of herringbone structure in Type II bursts. In: Kundu, M.R., Gergely, T.E. (eds.) *Radio Physics of the Sun, IAU Symposium* **86**, 241–245.
- Vršnak, B., Cliver, E.W.: 2008, Origin of Coronal Shock Waves. Invited Review. *Solar Phys.* **253**, 215–235. doi:10.1007/s11207-008-9241-5.
- Yashiro, S., Michalek, G., Akiyama, S., Gopalswamy, N., Howard, R.A.: 2008, Spatial Relationship between Solar Flares and Coronal Mass Ejections. *Astrophys. J.* **673**, 1174–1180. doi:10.1086/524927.
- Zajtsev, V.V., Zlotnik, E.Y., Mann, G., Aurass, H., Klassen, A.: 1998, Efficiency of electron acceleration by shock waves in the solar corona according to observational data on the fine structure of type II radio bursts. *Radiophysics and Quantum Electronics* **41**, 107–114. doi:10.1007/BF02679627.
- Zucca, P., Carley, E.P., McCauley, J., Gallagher, P.T., Monstein, C., McAteer, R.T.J.: 2012, Observations of Low Frequency Solar Radio Bursts from the Rosse Solar-Terrestrial Observatory. *Solar Phys.* **280**, 591–602. doi:10.1007/s11207-012-9992-x.

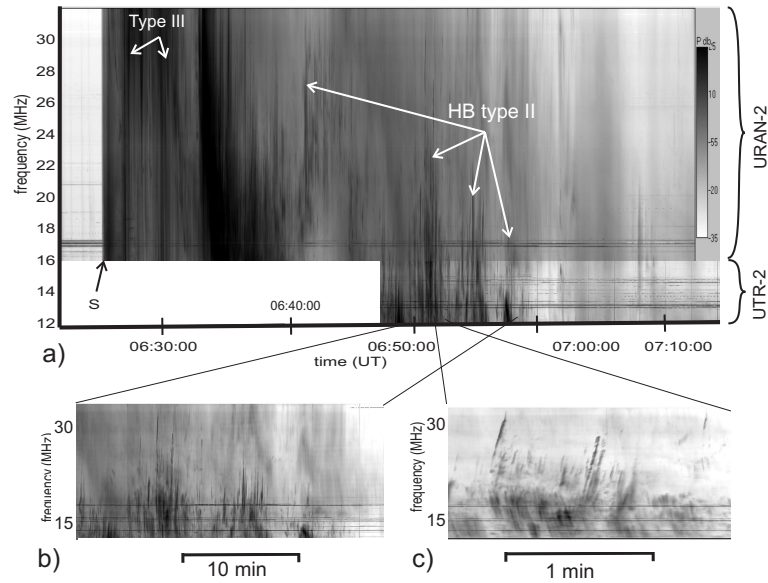


**Figure 1.** Dynamic spectra of: the whole event (a), the wavelike backbone (b) and separate HB sub-bursts (c).

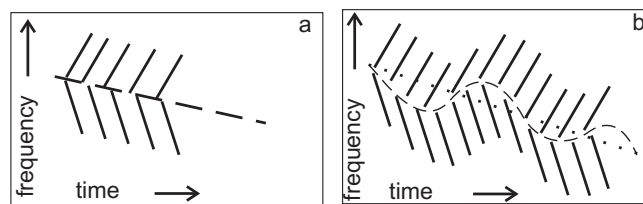


**Figure 2.** Schematic view of normal HB type II (a) and type II burst with the wavelike backbone (b)

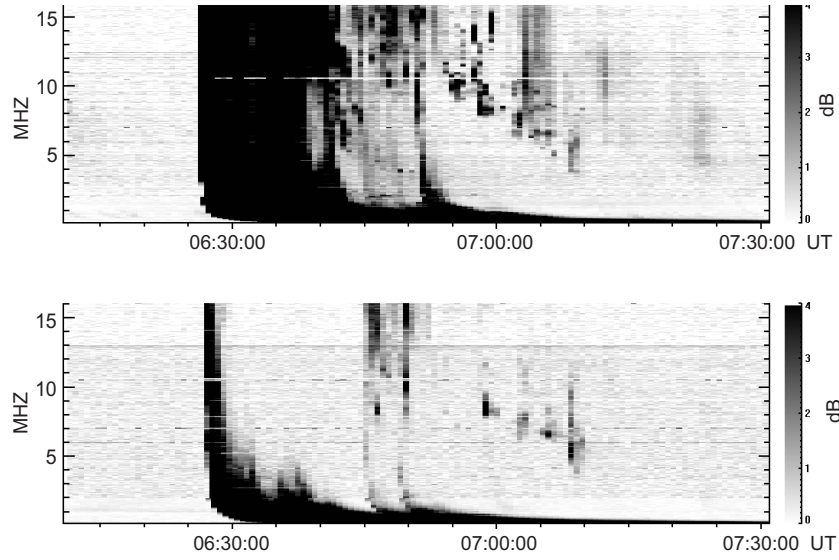


**Figure 3.** Type II burst from STEREO-A (top panel) and STEREO-B spacecraft (bottom panel).

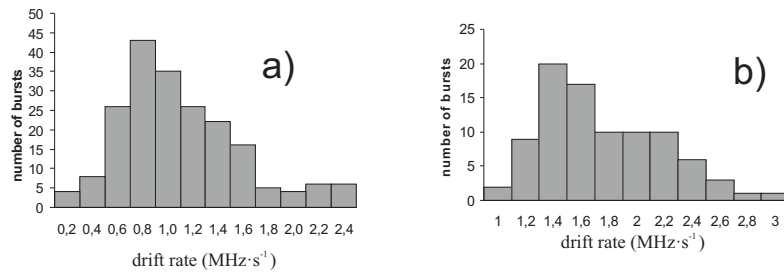


**Figure 4.** Distributions by the frequency drift rates of the forward (a) and the reverse HB sub-bursts (b).

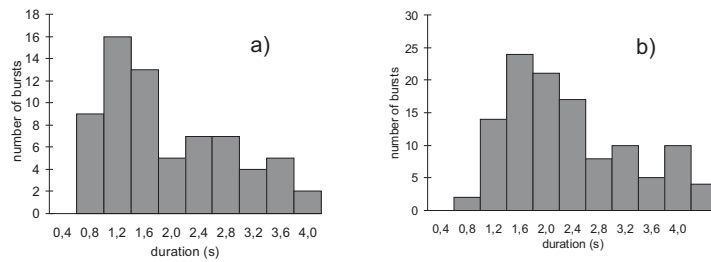


**Figure 5.** Distributions by the instant durations of the forward HB sub-bursts (a) and the reverse HB sub-bursts (b).

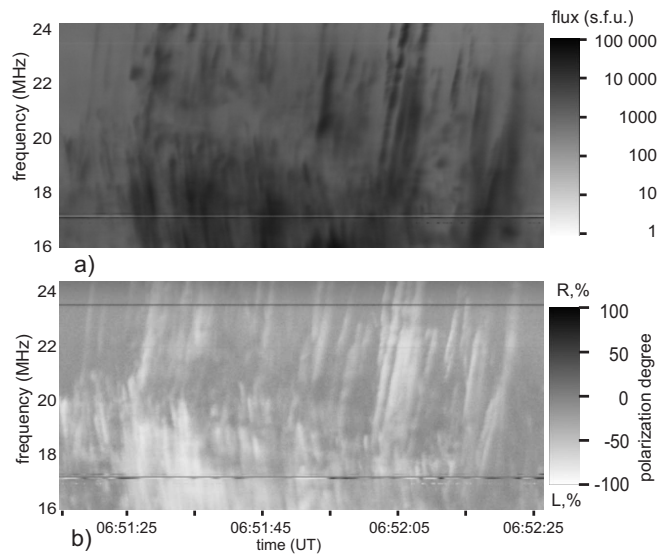


**Figure 6.** Fragments of the power (a) and the polarization spectra of the HB structure (b).

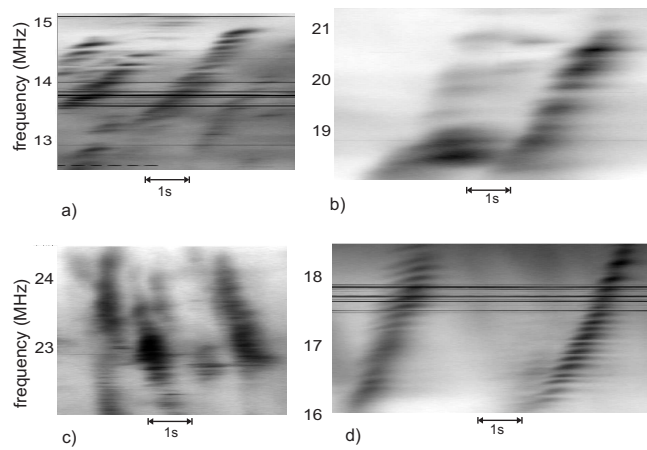


**Figure 7.** The fine frequency structure of the HB sub-bursts.

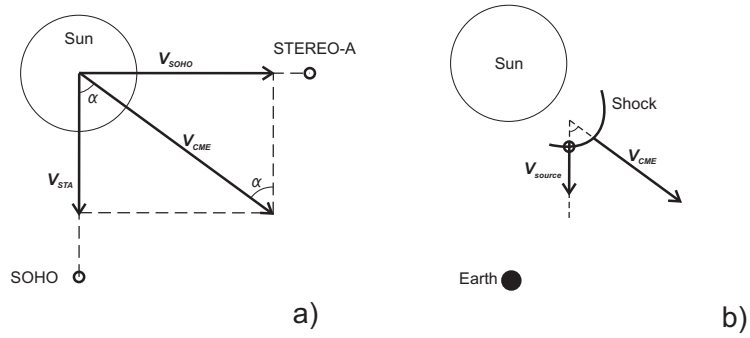


**Figure 8.** The geometry of CME speed detection (a) and schematic view of the type II source movement (b).



